



1 **Rapid formation of intense haze episode in Beijing**

2

3 Yonghong Wang^{1,2}, Yuesi Wang^{1,5}, Guiqian Tang¹, Tao Song¹, Putian Zhou², Zirui
4 Liu¹, Bo Hu¹, Dongsheng Ji¹, Lili Wang¹, Xiaowan Zhu¹, Chao Yan², Mikael Ehn²,
5 Wenkang Gao¹, Yuepeng Pan¹, Jinyuan Xin¹, Yang Sun¹, Veli-Matti Kerminen²,
6 Markku Kulmala^{2,3,4} and Tuukka Petäjä^{2,3,4}

7

8 ¹State Key Laboratory of Atmospheric Boundary Layer Physics and Atmospheric
9 Chemistry (LAPC), Institute of Atmospheric Physics, Chinese Academy of Sciences,
10 Beijing 100029, China

11

12 ²Institute for Atmospheric and Earth System Research / Physics, Faculty of Science,
13 P.O.Box 64, 00014 University of Helsinki, Helsinki, Finland

14

15 ³Joint international research Laboratory of Atmospheric and Earth SysTem sciences
16 (JirLATEST), Nanjing University, Nanjing, China

17

18 ⁴Aerosol and Haze Laboratory, Beijing Advanced Innovation Center for Soft Matter
19 Science and Engineering, Beijing University of Chemical Technology (BUCT),
20 Beijing, China

21 ⁵Centre for Excellence in Atmospheric Urban Environment, Institute of Urban
22 Environment, Chinese Academy of Science, Xiamen, Fujian 361021, China

23

24

25 Corresponding authors: Yuesi Wang and Markku Kulmala

26 E-mail: wys@mail.iap.ac.cn; markku.kulmala@helsinki.fi

27

28

29 Submitted to: Atmospheric Chemistry and Physics

30

31

32



33 **Keywords:** PM_{2.5}, Mixing layer height, Turbulent kinetic energy, vertical
34 measurement, feedback

35

36 **Abstract**

37

38 Although much efforts have been put on studying air pollution, our knowledge on
39 the mechanisms of frequently occurred intense haze episodes in China is still limited.
40 In this study, using three years of measurements of air pollutants at three different
41 height levels on a 325-meter Beijing meteorology tower, we found that a positive
42 particulate matter-boundary layer feedback mechanism existed at three vertical
43 observation heights during intense haze polluted periods within the mixing layer. This
44 feedback was characterized by a higher loading of PM_{2.5} with a shallower mixing
45 layer. Measurements showed that the feedback was related to the decrease of solar
46 radiation, turbulent kinetic energy and thereby suppression of the mixing layer. The
47 feedback mechanism can explain the rapid formation of intense haze episodes to some
48 extent, and we suggest that the feedback mechanism should be considered in air
49 quality models for better predictions.

50 **1. Introduction**

51 With the rapid economic growth and urbanization, an increasing frequency of haze
52 episodes along with the air pollution has become of great concern in China during the
53 last decade (Cao et al., 2016; Huang et al., 2014; Kulmala, 2015; Wang et al., 2014;
54 Wang et al., 2015). For example, during December 2016 a series of intense haze
55 episodes took place in Eastern China, characterized by surface PM_{2.5} concentrations
56 exceeding 500 $\mu\text{g m}^{-3}$ in several measurement sites in Beijing and its surrounding sites
57 (http://www.mep.gov.cn/gkml/hbb/qt/201701/t20170102_393745.htm). Severe air
58 pollution has serious effects on human health. A recent study reported that the
59 particulate matter has significantly decreased the life span of residents as many as 5.5
60 years in Northern China (Chen et al, 2013). In a global scale, the air pollution was
61 estimated to cause over 3 million premature deaths every year (Lelieveld et al., 2015).

62 Increased emissions from fossil fuel combustion due to vehicle traffic, industrial
63 activities and power generation, along with exceptionally strong secondary aerosol
64 formation, were thought to be responsible for these haze episodes (Cheng et al., 2016;
65 Huang et al., 2014; Pan et al., 2016; Petäjä et al., 2016; G Wang et al., 2016a; Zhang



66 et al., 2015; Zhao et al., 2013). Meanwhile, the formation of intense haze episodes
67 was considered to be affected by meteorological conditions (Wang et al., 2014; Quan
68 et al., 2013; Wang et al., 2016b; Zheng et al., 2016). For example, the mixing layer
69 height is a key parameter that constrains the dilution of surface air pollution, and the
70 development of mixing layer is highly related to the amount of solar radiation
71 absorbed by the air and reaching the surface (Ding et al., 2016; Stull, 1988; Sun et al.,
72 2013; Tang et al., 2016; Wilcox et al., 2016).

73 In this study, using unique measurements on the Beijing 325-meter-high
74 meteorology tower, we present direct evidence on the feedback that relates the
75 decreasing mixed layer height with increasing particulate matter concentrations, and
76 this feedback is critical to the formation of intense haze episodes in Beijing.

77

78 2. Methods

79 2.1 Calculation of mixing layer height with ceilometer

80 The mixing layer height was measured with the enhanced single-lens ceilometers (CL 31,
81 Vaisala, Finland), which utilized the strobe laser lidar technique (910 nm) to measure the
82 attenuated backscattering coefficient profiles. Detection range of the CL31 is 7.6 km with the
83 report period of 2-120 s. Detail information can be found in previous studies (Tang et al., 2016).
84 Since the distribution of particle concentrations is uniform in the mixing layer and has significant
85 differences between the mixing layer and free atmosphere, the height at where a sudden change
86 exists in the attenuated backscattering coefficient profile indicates the top of the mixing layer
87 height (Münkel et al., 2007). The Vaisala software product BL-VIEW was used to determine the
88 mixing layer height by finding the position with the maximum negative gradient ($-d\beta/dx$) in the
89 attenuated backscattering coefficient profiles as the top of the mixing layer (Tang et al.,
90 2016; Münkel et al., 2007).

91 2.2 Measurements of energy flux at 325m Beijing meteorology tower

92 The turbulent fluxes of sensible heat (Q_H), latent heat (Q_E) and The turbulence kinetic energy
93 (TKE) were measured at 140m level using eddy covariance technique. The raw data (10 Hz) of
94 wind components (u, v and w) and sonic temperature (T_s) recorded with three-dimensional sonic
95 anemometers (Model CSAT3, Campbell Scientific Inc., Logan, Utah, USA) and of water vapor



96 concentrations (q) with open-path infrared gas analyzers (Model LI-7500, LiCor Inc., Lincoln,
97 Nebraska, USA). The fluxes of heat (Q) were calculated as the covariance between the
98 instantaneous deviation or fluctuations of vertical velocity (w'_i) and their respective scalar (s'_i)
99 averaged over a time interval of 30 min:

$$100 \quad Q = \overline{w's'} = \frac{1}{N} \sum_{i=1}^N w's'$$

101 Where the over-bar denotes a time average, N is the number of samples during the averaging time
102 and the fluctuations are the differences between the instantaneous readings and their respective
103 means. The TKE were calculated as follows (Stull, 1988):

$$104 \quad \frac{\text{TKE}}{m} = \frac{1}{2} (\overline{u'^2} + \overline{v'^2} + \overline{w'^2}) = \bar{e}$$

105 where m is the mass (kg), e is the TKE per unit mass ($\text{m}^2 \text{s}^{-1}$). A more detailed description of the
106 calculation and post processing of flux is provided in Song et al. (2013).

107 2.3 Measurements of $\text{PM}_{2.5}$ concentration and gases in the 325m Beijing meteorology tower.

108 The mass concentration of $\text{PM}_{2.5}$ at 8m, 120m and 280m observation platform were measured
109 with three TEOM RP1400 simultaneously. (Thermo Scientific, <http://www.thermoscientific.com>).
110 The resolution and precision of the instrument for one-hour was of $0.1 \mu\text{g m}^{-3}$ and $\pm 1.5 \mu\text{g m}^{-3}$.
111 The filters were exchanged when the loading rates were approximately to 40% and the flow ratio
112 were monitored and calibrated monthly. The volume mixing ratios of ozone and NO_x were
113 measured with 49i and 42i (Thermal Environment Instruments (TEI) Inc.), respectively. Detailed
114 introduction can be found in Wang et al. (2014).

115 2.4 Other supporting measurements

116 Total solar radiation was measured with a direct radiometer (TBQ-2, Junzhou, China). Direct
117 radiation was measured with a direct radiometer (TBS-2, Junzhou, China). UV radiation in the
118 range of 400nm-220nm was measured using CUV3 radiometer (USA). The estimated experiment
119 error for the three instruments are 3%, 1% and 2%, respectively (Hu et al., 2012). The original
120 data were obtained at one-minute intervals and the hourly average values were used in this study.
121 The chemical composition of organic, sulphate, nitrate, ammonium and chloride in non-refractory
122 submicron aerosol were measured with an Aerodyne High-Resolution Time-of-Flight Aerosol
123 Mass Spectrometer (HR-ToF-AMS, Aerodyne Research Inc., Billerica, MA, USA) (DeCarlo et al.,
124 2006). Detailed information about instrument, calibration and data process have been introduced
125 by Zhang et al. (2014).

126 3 Results and Discussion



127 A typical intense haze episode occurred during the heating season in urban Beijing
128 during 17 to 22 November 2010. This episode was associated with synoptic
129 stagnation in the North China Plain (Figure S1) and was characterized by low wind
130 speeds and irregular wind direction (Figure 1). Several meteorological variables had
131 distinct temporal patterns during different stages of pollution, including reduced solar
132 radiation and surface temperatures and increased relative humidity during the most
133 intense presence of haze (Fig. 1) The temporal patterns of PM_{2.5} concentrations were
134 very similar at the two lower measurements heights (8 m and 120 m, Fig. 1d), even
135 though the concentration was clearly the highest close to the surface. The PM_{2.5}
136 concentration measured at 280 m behaved in a different way, especially during the
137 most intense period of the haze when the mixed layer height was very low (Fig. 1e).
138 The decoupling of the 280-m platform from the other two lower ones at low mixed
139 layer heights is apparent in our 3-year measurement data set, especially when
140 comparing O₃ and NO_x concentrations between the three measurement platforms
141 (Figs. S2 and S4). During the haze period, the maximum PM_{2.5} concentrations at 8,
142 120 and 280 m were 505, 267 and 339 g m⁻³, respectively. The higher maximum
143 concentration at 280 m compared with 120 m can be ascribed to the transport of
144 pollutants from surrounding regions of Hebei and Tianjin Provinces typical for
145 polluted periods (Sun et al., 2013). The mixing layer height varied from 130 m to
146 1640 m during the haze episode, ranging between about 200 and 500 m during the
147 most intense period of the haze period on 18 November 2010 (Fig. 1e).

148 The vertical distribution of attenuated backscatter density obtained from
149 ceilometer measurements indicate vertical mixing conditions accompanied with an
150 inversion layer and high relative humidity in the surface as shown in Figure 2. The
151 strong inversion and high relative humidity occurred on morning of 18 November
152 2010, with a lapse rate of 2K / 100 m, relative humidity of 78% and north-direction
153 wind speed of around 2 m / s detected by the vertical sounding. The turbulent kinetic
154 energy at 140 m was reduced to around 0.1~0.7 m²/s² due to decreased solar radiation,
155 as shown in Figure1(a). In this manner, the development of a mixing layer was
156 significantly suppressed during the intense haze episode.

157 In order to demonstrate how the mixing layer height modifies PM_{2.5}
158 concentrations, we used three years of simultaneous winter-time air pollutant
159 measurements in the Beijing tower at 8 m, 120 m and 280 m platforms. We divided



160 the observed $PM_{2.5}$ concentrations into highly-polluted and less-polluted conditions
161 using a threshold value of $75 \mu\text{g m}^{-3}$ for $PM_{2.5}$ to distinguish between these conditions.
162 This is consistent with Chinese Environment Protection Bureau definition of a haze
163 pollution events. With this threshold value, we found that 31% and 69% of total
164 measurement time corresponded to highly-polluted and less-polluted conditions,
165 respectively. We plotted the $PM_{2.5}$ data as a function of the mixing layer height at the
166 three observation heights during both highly-polluted and less-polluted conditions and
167 fitted an exponential curve to these data (Figure 3). The $PM_{2.5}$ concentration has a
168 clear anti-correlation with the mixing layer height during the intense haze episodes.
169 At all measurement heights, the $PM_{2.5}$ concentration increased as the mixing layer
170 height decreased, and this pattern was very strong under polluted conditions (Figure
171 3). It is worth noting that the increase was mainly from the $PM_{1-2.5}$ fraction that
172 increased from 42% to 65% as mixing layer height decreased from more than 1400 m
173 to lower than 300 m (Figure S3b). A major portion of particulate mass between 1 and
174 $2.5 \mu\text{m}$ originates from secondary aerosol formation processes in urban air (Wang et
175 al., 2014; Zhang et al., 2015). The reduction in solar radiation due to these fine
176 particle matters reaching the surface reduces the turbulent kinetic energy and the
177 development of mixing layer, as shown in Figure 4.

178 We assign part of the observed increase in $PM_{2.5}$ and simultaneous decrease in
179 the mixing layer height to a positive feedback from particulate matter-mixing layer
180 interaction (Petäjä et al. 2016, Ding et al. 2016), which occurred at the same time as
181 primary emissions and secondary formation were confined into a smaller volume of
182 air. The feedback occurred at all the three observation platforms and was most
183 intensive at 8 m. In an urban environment, NO_x originates mainly from local
184 anthropogenic emissions, whereas the sources of particulate matter include both
185 primary emissions and secondary formation (Ehn et al., 2014; Jimenez et al., 2009;
186 Zhang et al., 2015; Zhao et al., 2013). As shown in Figure S4, the median NO_x
187 concentration at 8 m was 250% higher under highly-polluted conditions compared
188 with less-polluted conditions as the mixing layer height decreased to 100-200 m,
189 while the corresponding number for the $PM_{2.5}$ concentration was 360%.

190 The increase of the $PM_{2.5}$ concentration from less-polluted to highly-polluted
191 conditions is mainly due to concentrated particulate matter caused by a decreased
192 mixing layer height, which is accompanied by primary particle emissions, secondary



193 aerosol formation and feedback from particulate matter-mixing layer height
194 interactions. Compared with the increased amounts of NO_x, we can roughly estimate
195 that in maximum 110% of the increased PM_{2.5} originates from secondary aerosol
196 formation processes in this study. Of the remaining 250% of the PM_{2.5} increase,
197 potentially a large fraction originates from particulate matter-mixing layer height
198 interactions, but we cannot quantify this fraction at the moment.

199

200 4 Conclusions

201 The development of mixing layer height in an urban city is affected by the
202 intensity of incoming solar radiation and by anthropogenic heating in the city. Our
203 measurement at the 325-meter meteorology tower showed that the solar and
204 ultraviolet radiation reaching the surface decrease considerably at increased pollution
205 levels., which leads to further increases in concentrations of PM_{2.5} and its precursor
206 gases from both direct emissions and secondary formation. This feedback mechanism
207 may be an important reason for rapid increase of particulate matter from moderate-
208 polluted conditions to periods of intense pollution in an urban atmosphere. The
209 particulate matter-mixing layer height feedback is probably a critical factor for the
210 formation of intense haze periods in Beijing and other polluted cities.

211 Acknowledgements

212 This work was supported by the Ministry of Science and Technology of China (No:
213 2017YFC0210000), the National Research Program for key issues in air pollution
214 control(DQGG0101) and Academy of Finland via Center of Excellence in
215 Atmospheric Sciences.

216 Competing financial interests

217 The authors declare no competing financial interests.

218 Author contributions



219 M.K, Y.S.W, T.P and Y.H.W, have the original idea. Y.S.W, G.T, T.S, Z.L, B.H,
220 L.W, X.Z, D.J, W.G and Y.S conducted the longtime measurements and provided the
221 data. Y.H.W, G.T, S.T, P.Z, M.E, C.Y, V.K, T.P and M.K interpreted the data and
222 plotted the figures. Y.H.W wrote the manuscript, with contribution from all co-
223 authors.

224

225 **References**

- 226 Cao, C., X. Lee, S. Liu, N. Schultz, W. Xiao, M. Zhang, and L. Zhao, Urban heat
227 islands in China enhanced by haze pollution, *Nature Communications*, 7, 12509,
228 doi:10.1038/ncomms12509, 2016.
229 <http://www.nature.com/articles/ncomms12509#supplementary-information>.
- 230 Cheng, Y., et al. Reactive nitrogen chemistry in aerosol water as a source of sulfate
231 during haze events in China, *Science Advances*, 2(12), doi:10.1126/sciadv.1601530,
232 2016.
- 233 Ding, A. J., et al. Enhanced haze pollution by black carbon in megacities in China,
234 *Geophysical Research Letters*, 43(6), 2873-2879, doi:10.1002/2016gl067745.
- 235 Ehn, M., et al. (2014), A large source of low-volatility secondary organic aerosol,
236 *Nature*, 506(7489), 476-479, doi:10.1038/nature13032,2016.
- 237 Huang, R.-J., et al. High secondary aerosol contribution to particulate pollution
238 during haze events in China, *Nature*, 514(7521), 218-222, doi:10.1038/nature13774,
239 2014.
240 [http://www.nature.com/nature/journal/v514/n7521/abs/nature13774.html#supplement](http://www.nature.com/nature/journal/v514/n7521/abs/nature13774.html#supplementary-information)
241 [ary-information](http://www.nature.com/nature/journal/v514/n7521/abs/nature13774.html#supplementary-information).
- 242 Jiandong, Wang., et al., Impact of aerosol–meteorology interactions on fine particle
243 pollution during China’s severe haze episode in January 2013, *Environmental*



- 244 Research Letters, 9(9), 094002, 2014.
- 245 Jimenez, J. L., et al., Evolution of Organic Aerosols in the Atmosphere, *Science*,
246 326(5959), 1525-1529, doi:10.1126/science.1180353, 2009.
- 247 Kulmala, M., China's choking cocktail, *Nature*, 526, 497-499, 2015.
- 248 Lelieveld, J., J. S. Evans, M. Fnais, D. Giannadaki, and A. Pozzer, The contribution of
249 outdoor air pollution sources to premature mortality on a global scale, *Nature*,
250 525(7569), 367-371, doi:10.1038/nature15371, 2015.
- 251 Pan, Y., et al., Redefining the importance of nitrate during haze pollution to help
252 optimize an emission control strategy, *Atmospheric Environment*, 141, 197-202,
253 doi:<http://dx.doi.org/10.1016/j.atmosenv.2016.06.035>, 2016.
- 254
- 255 Petäjä, T., et al., Enhanced air pollution via aerosol-boundary layer feedback in China,
256 *Scientific Reports*, 6, 18998, doi:10.1038/srep18998
257 <http://www.nature.com/articles/srep18998#supplementary-information>, 2016.
- 258
- 259 Quan, J., Y. Gao, Q. Zhang, X. Tie, J. Cao, S. Han, J. Meng, P. Chen, and D. Zhao,
260 Evolution of planetary boundary layer under different weather conditions, and its
261 impact on aerosol concentrations, *Particuology*, 11(1), 34-40,
262 doi:<http://dx.doi.org/10.1016/j.partic.2012.04.005>, 2013.
- 263
- 264 Stull, R. B., *An Introduction to Boundary Layer Meteorology*, Kluwer Academic
265 Publishers, Dordrecht, 1988.
- 266
- 267 Sun, Y., T. Song, G. Tang, and Y. Wang, The vertical distribution of PM_{2.5} and
268 boundary-layer structure during summer haze in Beijing, *Atmospheric Environment*,
269 74, 413-421, doi:<http://dx.doi.org/10.1016/j.atmosenv.2013.03.011>, 2013.
- 270
- 271 Tang, G., et al., Mixing layer height and its implications for air pollution over Beijing,
272 China, *Atmos. Chem. Phys.*, 16(4), 2459-2475, doi:10.5194/acp-16-2459-2016, 2016.
- 273
- 274 Wang, G., et al., Persistent sulfate formation from London Fog to Chinese haze,
275 *Proceedings of the National Academy of Sciences*, 113 (48), 13630-13635,
276 doi:10.1073/pnas.1616540113, 2016.



277

278 Wang, X., K. Wang, and L. Su, Contribution of Atmospheric Diffusion Conditions to
279 the Recent Improvement in Air Quality in China, *Scientific Reports*, 6, 36404,
280 doi:10.1038/srep36404,

281 <http://www.nature.com/articles/srep36404#supplementary-information>, 2016.

282

283 Wang, Y., L. Yao, L. Wang, Z. Liu, D. Ji, G. Tang, J. Zhang, Y. Sun, B. Hu, and J.
284 Xin, Mechanism for the formation of the January 2013 heavy haze pollution episode
285 over central and eastern China, *Science China Earth Sciences*, 57(1), 14-25,
286 doi:10.1007/s11430-013-4773-4, 2014.

287

288 Wang, Y. H., Z. R. Liu, J. K. Zhang, B. Hu, D. S. Ji, Y. C. Yu, and Y. S. Wang,
289 Aerosol physicochemical properties and implications for visibility during an intense
290 haze episode during winter in Beijing, *Atmos. Chem. Phys.*, 15(6), 3205-3215,
291 doi:10.5194/acp-15-3205-2015, 2015.

292

293 Wilcox, E. M., R. M. Thomas, P. S. Praveen, K. Pistone, F. A.-M. Bender, and V.
294 Ramanathan, Black carbon solar absorption suppresses turbulence in the atmospheric
295 boundary layer, *Proceedings of the National Academy of Sciences*, 113(42), 11794-
296 11799, doi:10.1073/pnas.1525746113, 2016.

297

298 Yuyu Chen, A. E., Michael Greenstone, and Hongbin Li, Evidence on the impact of
299 sustained exposure to air pollution on life expectancy from China's Huai River policy,
300 *PNAS* 110 (32), doi:doi:10.1073/pnas.1300018110, 2013

301

302 Zhang, R., G. Wang, S. Guo, M. L. Zamora, Q. Ying, Y. Lin, W. Wang, M. Hu, and
303 Y. Wang, Formation of Urban Fine Particulate Matter, *Chemical Reviews*, 115(10),
304 3803-3855, doi:10.1021/acs.chemrev.5b00067, 2015.

305

306 Zhao, B., S. X. Wang, H. Liu, J. Y. Xu, K. Fu, Z. Klimont, J. M. Hao, K. B. He, J.
307 Cofala, and M. Amann, NO_x emissions in China: historical trends and
308 future perspectives, *Atmos. Chem. Phys.*, 13(19), 9869-9897, doi:10.5194/acp-13-
309 9869-2013, 2013.



- 310
- 311 Zheng, G., F. Duan, Y. Ma, Q. Zhang, T. Huang, T. Kimoto, Y. Cheng, H. Su, and K.
312 He, Episode-Based Evolution Pattern Analysis of Haze Pollution: Method
313 Development and Results from Beijing, China, *Environmental Science & Technology*,
314 50(9), 4632-4641, doi:10.1021/acs.est.5b05593, 2016
- 315
- 316 DeCarlo, P. F., Kimmel, J. R., Trimborn, A., Northway, M. J., Jayne, J. T., Aiken, A.
317 C., Gonin, M., Fuhrer, K., Horvath, T., Docherty, K. S., Worsnop, D. R., and Jimenez,
318 J. L.: Field-Deployable, High-Resolution, Time-of-Flight Aerosol Mass Spectrometer,
319 *Analytical Chemistry*, 78, 8281-8289, 10.1021/ac061249n, 2006.
- 320 Hu, B., Wang, Y., and Liu, G.: Relationship between net radiation and broadband
321 solar radiation in the Tibetan Plateau, *Advances in Atmospheric Sciences*, 29, 135-
322 143, 10.1007/s00376-011-0221-6, 2012.
- 323
- 324 Münkkel, C., Eresmaa, N., Räsänen, J., and Karppinen, A.: Retrieval of mixing height
325 and dust concentration with lidar ceilometer, *Boundary-Layer Meteorology*, 124, 117-
326 128, 10.1007/s10546-006-9103-3, 2007.
- 327
- 328 Song, T., Sun, Y., and Wang, Y.: Multilevel measurements of fluxes and turbulence
329 over an urban landscape in Beijing, *Tellus B: Chemical and Physical Meteorology*, 65,
330 20421, 10.3402/tellusb.v65i0.20421, 2013.
- 331
- 332 Stull, R. B.: *An Introduction to Boundary Layer Meteorology*, Kluwer Academic
333 Publishers, Dordrecht, 1988.
- 334
- 335 Tang, G., Zhang, J., Zhu, X., Song, T., Münkkel, C., Hu, B., Schäfer, K., Liu, Z., Wang,
336 L., Xin, J., Suppan, P., and Wang, Y.: Mixing layer height and its implications for air
337 pollution over Beijing, China, *Atmos. Chem. Phys.*, 16, 2459-2475, 10.5194/acp-16-
338 2459-2016, 2016.
- 339
- 340 Wang, Y. H., Hu, B., Ji, D. S., Liu, Z. R., Tang, G. Q., Xin, J. Y., Zhang, H. X., Song,
341 T., Wang, L. L., Gao, W. K., Wang, X. K., and Wang, Y. S.: Ozone weekend effects
342 in the Beijing–Tianjin–Hebei metropolitan area, China, *Atmos. Chem. Phys.*, 14,



343 2419-2429, 10.5194/acp-14-2419-2014, 2014.

344

345 Zhang, J. K., Sun, Y., Liu, Z. R., Ji, D. S., Hu, B., Liu, Q., and Wang, Y. S.:

346 Characterization of submicron aerosols during a month of serious pollution in Beijing,

347 2013, Atmos. Chem. Phys., 14, 2887-2903, 10.5194/acp-14-2887-2014, 2014.

348

349

350

351

352

353

354

355

356

357

358

359

360

361

362

363

364

365

366

367

368

369

370

371

372

373

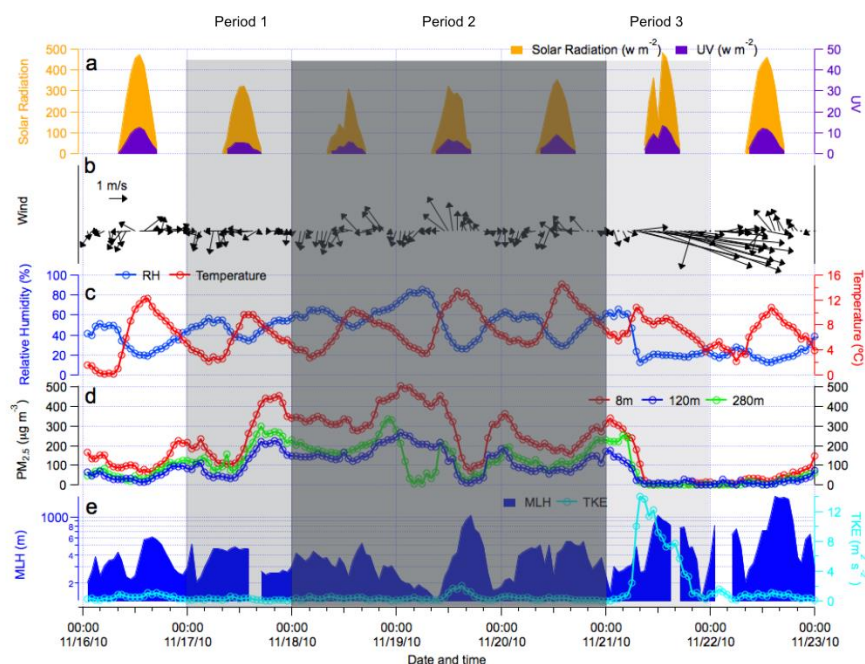
374

375



376

Figure captions

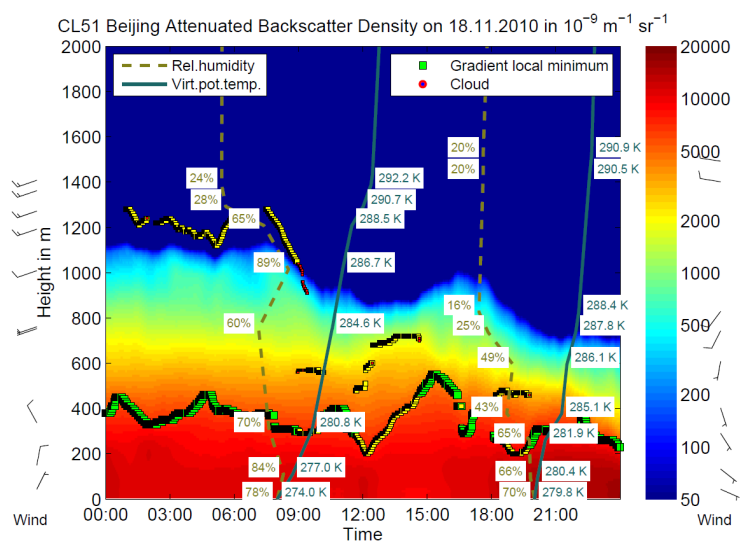


377

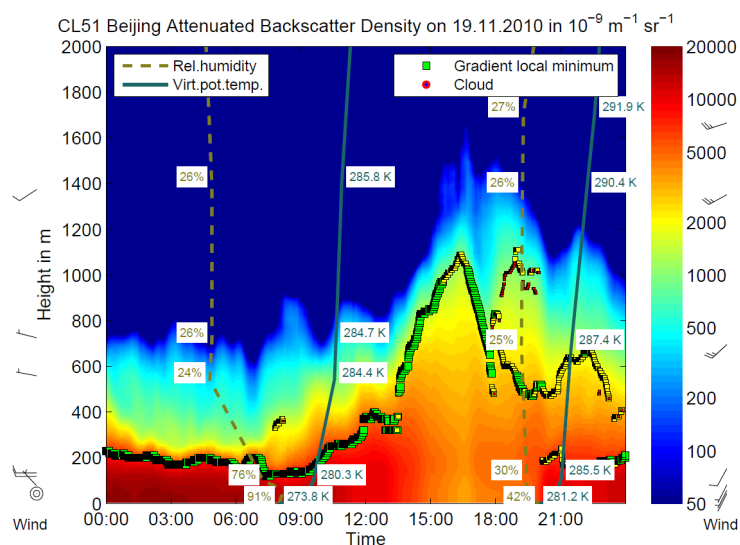
378

379 **Figure 1.** Measurements of (a) solar radiation and ultraviolet radiation at 8 m, (b)
380 wind speed and direction at 8 m, (c) relative humidity and air temperature at 8 m, (d)
381 mass concentration of PM_{2.5} at 8 m, 120 m and 280 m, (e) mixing layer height at 8 m
382 and turbulence kinetic energy at 140 m in the Beijing 325-meter meteorology tower
383 during an intensive air pollution episode in November of 2010. The evolution of the
384 air pollution episode can be divided into the period 1 (clean period to air pollution
385 accumulation period, period 2 (pollution period) and period 3 (pollution to clean
386 period).

387



388



389

390

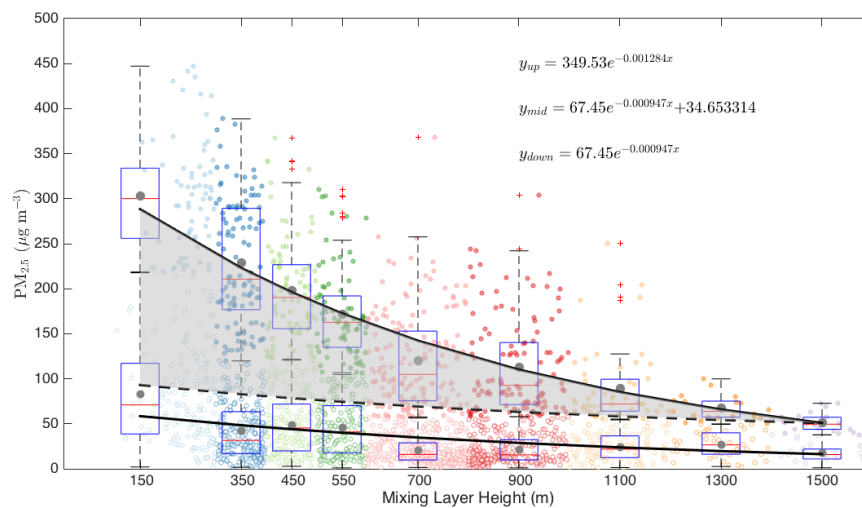
391 **Figure 2.** Observed attenuated backscatter density, calculated mixing layer height
 392 using ceilometer and vertical wind speed, wind direction, relative humidity, virtual
 393 potential temperature using sounding data during November 18 (top) and 19 (bottom).
 394 The black flag in the left and right side of the figures stand for vertical wind speed
 395 and wind direction obtained from sounding measurements at 08:00 and 20:00 of
 396 Beijing time, respectively. The circle in the left side of figure stands for calm wind.
 397 The dotted yellow lines and solid green lines stand for vertical distribution of virtual



398 potential temperature and relative humidity from sounding at 08:00 and 20:00,
399 respectively. The mixing layer height was determined from the local minimum of the
400 backscatter density gradient, and the colour in the figure stands for backscatter density
401 from ceilometer. From both figures, we can clearly see that mixing layer has
402 important role in regulating distribution of air pollutants.
403



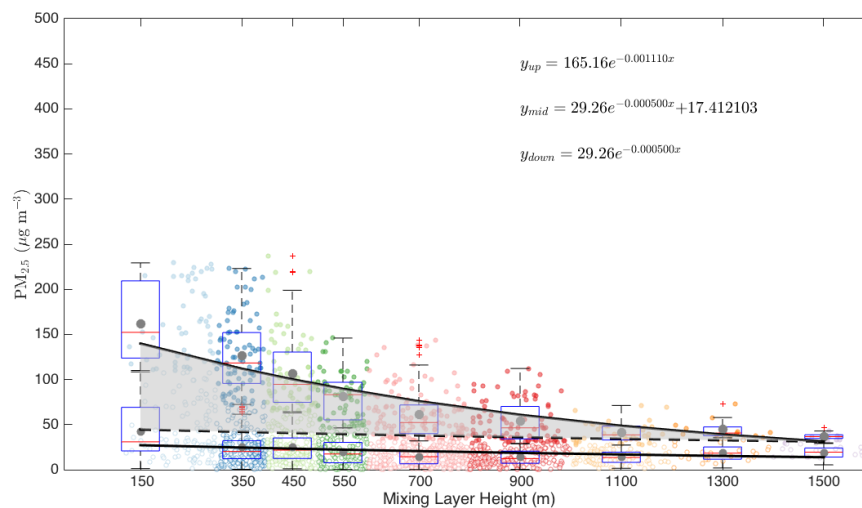
404



405

406

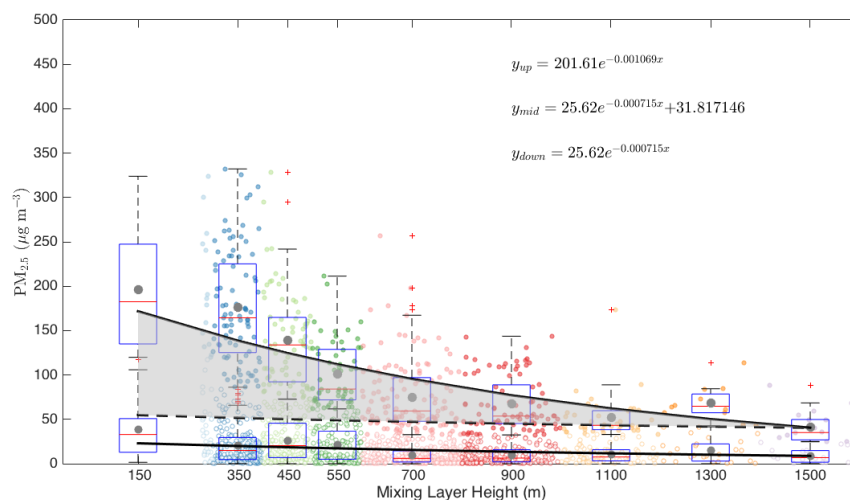
(a)



407

408

(b)



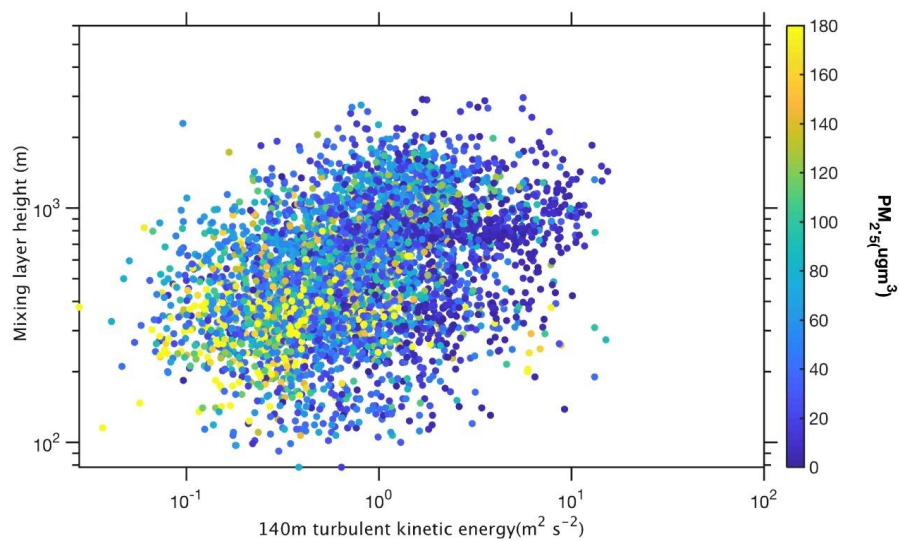
(c)

Figure 3. The variability of the PM_{2.5} mass concentration as a function of the mixing layer height at 8 m (a), 120 m (b) and 280 m (c). The data related to the upper fitting line represents PM_{2.5} concentrations larger than 75 $\mu\text{g m}^{-3}$, while the data related to the lower fitting line represents PM_{2.5} concentrations less than 75 $\mu\text{g m}^{-3}$. The dark grey points represent mean values; the red line represents median values. The shadowed area corresponds to an increased amount of PM_{2.5} with decreased mixing layer height assuming that PM_{2.5} has the same variation pattern under highly- polluted conditions as in less polluted time.

409
410
411
412
413
414
415
416
417
418
419
420
421
422
423
424
425
426
427
428
429
430



431
432
433
434
435
436
437
438
439
440
441



442
443
444
445

Figure 4. Turbulent kinetic energy at 140 m as a function of mixing layer height and $PM_{2.5}$ concentrations at 140 m.